

Theoretical Study to improve electrical and thermal efficiency of a photovoltaic-thermal hybrid system PV/T in the region of Algerian Sahara (Ouargla)

Kheira Djemoui^{1,2}, Djamel Benmenine^{1,4}, Soufiane Benhamida^{3,2}, Mohammed Elbar Soudani^{1,2}, Afak Benazzouz^{1,2}

Received: 02/01/2024; Accepted: 28/05/2024; Published: 12/06/2024

Abstract: Solar energy stands as one of the most significant renewable energy sources, with the sun's daily radiation potentially covering the global energy consumption for years. It offers a clean, pollution-free, inexhaustible, and widely available source of energy. Solar energy can be directly converted into electricity through photovoltaic cells or into heat via various solar collectors. Due to the low efficiency of photovoltaic (PV) stations resulting from the high surface temperature of solar cells, this study embarks on a theoretical exploration of a hybrid photovoltaic-thermal (PVT) system in the Ouargla region, characterized by its dry and hot summer climate, located at 31.15° longitude and 5.24° latitude.

Electricity is generated through solar cells, while heat is concurrently absorbed by a heat exchanger, enhancing the PV cells' efficiency by reducing their surface temperature and effectively utilizing the heat through a solar collector. We found that hybridization reduces the solar panel's temperature by about 30°C and increases the electrical efficiency by approximately 2.5% on a summer day.

Keywords: PVT system, hybridization, thermal convection, Thermal and electrical efficiency.

Introduction

Solar energy is a resource that is renewable, eco-friendly, and free to use on Earth, can partially meet energy requirements and help maintain ecological balance. Its utilization conserves traditional energy sources and protects the environment from degradation, marking it as a promising and sustainable energy resource. Solar energy is directly converted into electricity through photovoltaic cells. [1] However, most

solar radiation received by photovoltaic panels is not converted into electrical energy; only 15-20% is transformed into electricity, while the remainder causes an increase in the temperature of the PV cells' surfaces, negatively impacting their performance. [2], [3]

This temperature rise leads to a decrease in electrical efficiency and a reduction in their lifespan. [4] The low efficiency of PV systems at high temperatures remains a major barrier to adopting sustainable systems. [5] Maintaining the PV cells' temperature within an optimal range is crucial for efficient operation. Cooling techniques for PV panels have proven to be an effective method to reduce the high temperatures of PV cells and enhance their electrical efficiency. [6] The hybrid PVT system is among the most efficient technologies for converting sunlight into heat and electricity. [7]

The PVT system, a novel arrangement that combines photovoltaic panels with a thermal solar collector in a single system, produces both electrical and thermal energy simultaneously. [8] The hybrid PV/T system consists of photovoltaic solar panels for electricity generation paired with a heat-absorbing panel behind the PV panels, which extracts heat and transfers it via a fluid

1 Laboratory of New and Renewable Energies
Development in Arid Zones, University of Ouargla.

2 Department of Physics, Faculty of Mathematics and
Science material,

Kasdi Merbah University Ouargla, Ouargla 30000
Algeria

3 Laboratory of Radiation and Plasma and Surface
Physics laboratory, University Kasdi Merbah Ouargla

4 Department of Renewable Energy, Faculty of
hydrocarbons, renewable energies, earth and universe
sciences, University of Kasdi Merbah –Ouargla

Email : djemoui.kheira@univ-ouargla.dz

passing through pipes, thereby reducing the solar panels' temperature and increasing their efficiency. Researchers discovered the hybrid PV/T system, with the first projects related to the PV/T system launched in 1973, Boer and Tamm proposed the first work on air-type PV/T systems, called Solar One House, which allowed direct conversion of sunlight into electricity and heat for domestic use [9]. Subsequently, researchers continued to explore PV/T systems. Grag and Agarwal created a simulation model to examine how a hybrid PVT air heating system works and how it performs based on its design outcomes. [10], finding that its efficiency greatly depends on its design temperatures, with a single glass cover potentially leading to increased heat collection compared to double glazing under certain critical points. The panel-and-tube covered system for tap water heating was found to be promising by De Vries, Zondag, and others in their testing of a PVT solar boiler with a water storage tank. [11]-[12]

Calogero studied the monthly performance of an unglazed hybrid PVT system under forced operation conditions in South Cyprus, noting an increase in the system's average annual efficiency from 2.8% to 7.7% with a efficiency of 31.7% [13]. Tiwari and Sodha developed a thermal model for an integrated photovoltaic and thermal solar energy system (IPVTS) and compared it with the traditional solar water heater model by Huang and al., with simulation predicting a daily primary energy saving efficiency of about 58%, Which is well consistent with the experimental value 61.3% obtained by Huang and al. [14] Trip Anagnostopoulos improved the current system by installing an unglazed dual PVT system that has both water and air cooling modes, and discovered that water pipes connected to the PV back surface improve thermal efficiency. [15]

Shahsavari and Ameri developed and evaluated a PVT air collector that could be directly coupled with or without glass in Kerman, Iran, [16]. Finalizing that installing a glass cover on photovoltaic panels enhances thermal efficiency while diminishing electrical efficiency. Bakar and others have modified the photovoltaic thermal solar collector design by adding a tapered circular copper tube below the photovoltaic panel, [17] which allows for both hot air and water to be provided and boosts the electrical output per unit compared to regular photovoltaic panels. Vats and others analyzed various photovoltaic materials for a BIPV system with air ducts and found that a packing factor of 0.62 has better thermal and electrical efficiency than a packing factor of 0.83. [18]

Tyagi and al. conducted a study on a solar air heater under three different conditions: without phase change material (PCM) - paraffin wax, with PCM, and with hither oil. The study demonstrated that the efficiency with paraffin wax was the highest compared to the other two conditions [19]. Tawfik and al, manufactured and studied a new improved design of a hybrid solar energy collector for hot air supply, showing superior thermal and electrical efficiency compared to traditional air heaters, with a thermal performance of up to 48% [20]. Amori and al, tested various photovoltaic solar collectors under different configurations in outdoor conditions. A mathematical model was developed to predict the performance of these collectors [21]. In this study, Al-Alili et al, applied a photovoltaic system for air conditioning assistance using a hybrid dryer, indicating improved thermal comfort compared to a vapor compression system [22]. Li and al, designed and tested a new integrated stationary CPC-PV/T system. A mathematical model was developed to predict the photonic performance under outdoor situation and was verified using experimental results, showing excellence agreement. [23]

Gang and al designed and developed a novel thermal photovoltaic system based on heat pipes, compared to the existing water system, demonstrating better performance. [24] Zhang and al. introduced an innovative concept for integrating heat pipes into a Hybrid Photovoltaic Thermal system, was evaluated this system in outside conditions for seven consecutive days, showing better performance than the existing solar air system. [25]

Moradgholi and al. presented a new concept for cooling solar panels using a set of heat pipes, enhancing the system's electrical efficiency [26]. Ji and al. developed a new solar heat pump system (PVT-SAHP) combining a Rankine cooling cycle and a PVT collector, with results indicating photovoltaic efficiency and thermal efficiency of the evaporator around 12% and 50% respectively in China [27]. Nanofluids were used as a cooling liquid. [28]•[29]• [30]•[31]• [32]•[33]

Dubey and Tiwari identified and presented a PV/T-based solar water collector, concluding logical hinges as climatic conditions and design parameters, based on the observed absorption area. If the PV coverage area is reduced to one-third, the instantaneous efficiency increases from 33% to 64%. [34] Mishra and Tiwari examined a water-based PV/T system based on a fixed collector temperature, finding that fully covered photovoltaics were suitable for electricity generation,

and partially covered photovoltaics were reasonable for hot water generation .[35]

V. Tirupati Rao and Y. Raja Sekhar provided a detailed review of thermal absorption designs contributing to the cooling of the solar panel for the PV/T system [36]. Singgih Dwi Prasetyo, Aditya Rio Prabowo studied the thermal load of the photovoltaic cell layer using steady-state thermal ANSYS simulation, achieving significant electrical efficiencies for the photovoltaic cells, with the highest efficiency reaching 11.98%, and the thermal efficiency was 82.7%.[37] Chang and al. found that an increase in temperature causes a significant decrease in cell efficiency. Thus, the cell's performance is optimized by heat absorption, which can be used for building heating and other purposes. [38]

This paper aims to study a hybrid photovoltaic thermal system in the Ouargla region, located within the solar belt where the solar radiation flux reaches 2650 Kwh/year/m², with about 3500 hours of sunshine per year, making it a hub for solar energy. However, the high average temperatures during the summer months negatively affect the efficiency of photovoltaic cells.

To provide hot water in an isolated area, this study proposes a hybrid system consisting of an 8.76 m² solar panel integrated with a heat exchanger to feed a pump where electricity is generated, and in parallel, heat is absorbed by a heat exchanger. This results in an increase in the efficiency of the photovoltaic cells due to the reduction in the temperature of their surfaces, and the utilization of heat by the solar collector in heating water in a useful manner, all while taking into account the climatic and weather conditions (air temperature, solar radiation) of the region.

PVT System Model

Figure 1 illustrates the working principle of the PVT system, consisting of a photovoltaic panel, JAP6-72-320 / 4B, with the electrical characteristics of the photovoltaic panels provided by the manufacturer listed in Table 1 [39], covered with a glass cover hybridized with a heat exchanger in the form of a twisted copper tube containing fluid (water) attached to the photovoltaic cell and connected to thermal insulation.

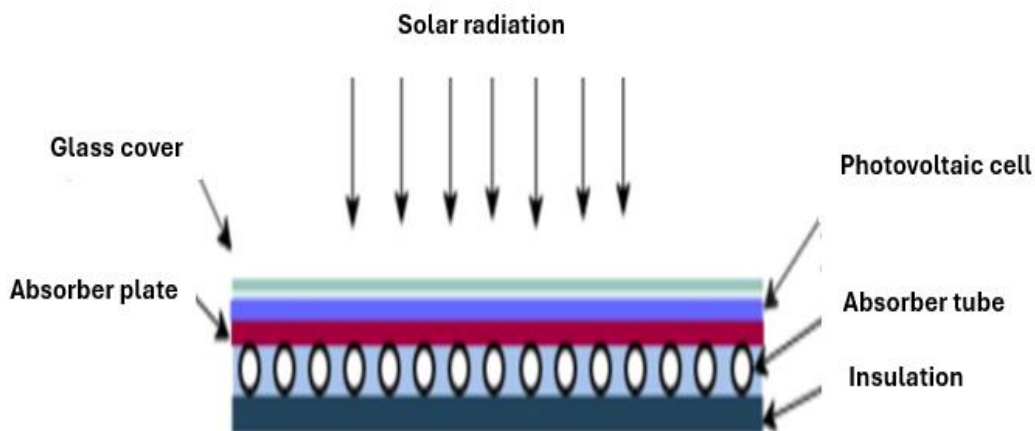


Figure 1: Model of the PVT system working principle.

Table 1: Quantities and characteristics of the solar photovoltaic unit JAP6-72-320 / 4B.

| Parameters | Variables | Values |
|--|----------------|---------|
| Maximum power at STC (P _m) | p _m | 320 W |
| Maximum power voltage (V _{mp}) | v _m | 37.38 V |
| Maximum power current (I _{mp}) | I _m | 8.56 A |

| | | |
|--|-----------|-------------|
| Open circuit voltage (V_{oc}) | V_{oc} | 46.22 V |
| Short-circuit current (I_{sc}) | I_{sc} | 9.06 A |
| Total series cells | N_s | 72 |
| Total parallel cells | N_p | 1 |
| Ideality factor of diode | A | 1.3 |
| Cell short circuit current temperature coefficient of I_{sc} | K_i | 0.058%/°C |
| Reference temperature | T_{ref} | 25 °C |
| Solar Irradiance | G_{ref} | 1000 at STC |

PVT System Layout

A typical layout of the PV/T system is given in Figure 2, showing the basic components of the PV/T system.

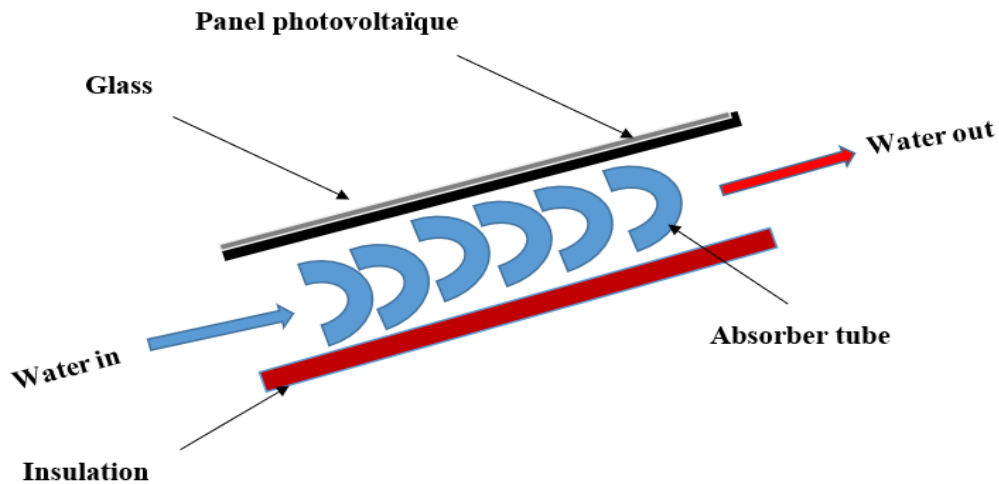


Figure 2: Typical layout of the PV/T system

Determining the Dimensions of the Solar Panel (Sizing)

To determine the necessary dimensions of the PV panel, we refer to the panel module model (JAP6-72-320 / 4BB) intended for operating a submersible pump

PS1800 C-SJ5-12 (Item No. 1163) in an isolated area, where the pump's power is 1600W and its operating voltage is $V_M = 94v$. [40]

From the data in Table 1 and information about the pump, we find the Quantities in Table 2 :

Table 2 Quantities and characteristics of the solar photovoltaic system.

| Parameters | Variables | Values |
|---------------------------|-----------|-------------------------|
| Area of a Single Cell | S | 0.024336 m ² |
| Voltage of a Single Cell | V_0 | 0.52v |
| Number of Cells in Series | N_s | 180 |

| | | |
|-------------------------------|----------|-----------|
| Power of a Single Solar Cell | P_0 | 4.44w |
| Total Number of Cells | N | 360 |
| Current of a Single Cell | I_0 | 0.12A |
| Number of Cells in Parallel | N_p | 2 |
| Total Area of the Solar Panel | S_{PV} | $8.76m^2$ |

Hence, to operate the pump, 180 cells must be installed in series and 2 in parallel, with a total of 360 cells.

The electrical characteristics (V – I) of the PV system composed of a number of solar cells connected in series and parallel shown in Figure 3, are determined based on the following equations:

Mathematical Model for the Photovoltaic (PV) System:

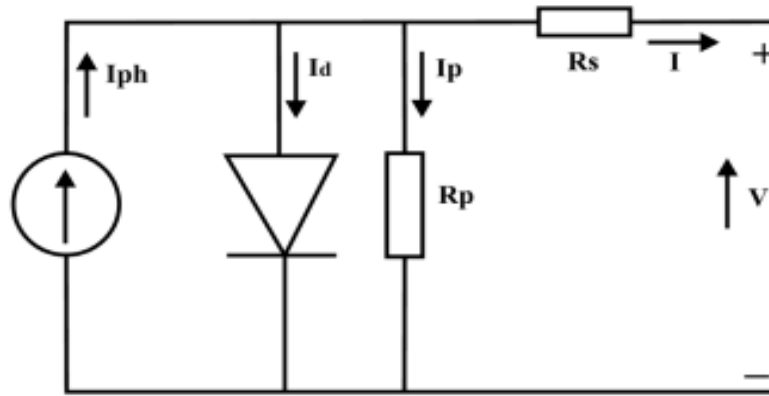


Figure 3: Equivalent circuit for the solar cell PV [41].

The output current of the solar cell is described in Equation (1). [42]

$$I = I_{ph} - I_d \quad (1)$$

The diode current is given in Equation (2).

$$I_d = I_s \left[\exp \left(\frac{q(V + IR_s)}{N_s K A T_0} \right) - 1 \right] \quad (2)$$

The reverse saturation current I_{rs} and the saturation current I_s are calculated using Equations (3) and (4), where the diode's ideal factor A and the energy gap E_g were obtained from the specified model, taken from the manufacturer of the specified unit.[43]

$$I_{rs} = I_{sc} / \left[\exp \left(\frac{qV_{oc}}{N_s K A T_0} \right) - 1 \right] \quad (3)$$

$$I_s = I_{rs} \left[\frac{T_0}{T_r} \right]^3 \exp \left[\left(\frac{qE_g}{AK} \right) \left(\frac{1}{T_r} - \frac{1}{T_0} \right) \right] \quad (4)$$

Hence, the output current resulting from the cell is shown in Equation (5) [44]

$$I_{ph} = [I_{sc} + K_i(T_0 - T_r)] * \frac{G}{G_{ref}} \quad (5)$$

Equation for Electrical Efficiency

The electrical efficiency is calculated according to the following Equation (6): [45]

$$\eta_{el} = \frac{VI}{GS_{pv}} \quad (6)$$

I is the output current and V is the output voltage of the PV solar cells and S_{pv} is the PV panel surface area.

Thermal Mathematical Model

The following assumptions are made for writing the energy balance equations for the PV/T collector model .Table 3 presented The parameters values of PV/T system

- Laminar flow
- Uniform temperatures on the top and back surfaces of the photovoltaic panel
- Neglecting the thickness of the absorbing tube
- Constant water velocity in the collector channel
- Considering the thermal insulation to be perfect with no heat loss
- One-dimensional heat transfer

Table 3: The parameters values of the PV/T collector.

| Layers | Parameters | Values |
|----------------|--|--|
| Air | λ_{air} Thermal conductivity [W/m K] v velocity of air [m/s] ρ_{air} Density [kg/m ³] μ_{air} Dynamic viscosity [kg m ⁻¹ s ⁻¹] | 0.0287 4 1.127 1.9.10 ⁻⁵ |
| PV glass-cover | λ_{pv} Thermal conductivity [W/m K] e_{pv} Thickness [m] ε emissivity Cp_{pv} Specific heat [J/kg K] α_{pv} Absorptivity ρ_{pv} Density [kg/m ³] l_{pv} Length of PV [m] | 1.15 0.01 0.95 3000 0.05 3000 6.24 |
| Absorber Tube | D diameter [m] L Length of tube [m] λ_{abst} Thermal conductivity [W/m K] ρ_{abst} Density [kg/m ³] Cp_{abst} Specific heat [J/kg K] | 0.012 16 54 8020 500 |
| Fluid(water) | \dot{m}_f water mass fow rate [kg/s] Cp_f Specific heat [J/kg K] λ_f Thermal conductivity [W/m K] | 0.1 4182 995 |
| Insulation | λ_i Thermal conductivity [W/m K] e_i Thickness [m] ρ_i Density [kg/m ³] | 0.02 0.015 |

| | | |
|--|--------------------------------|-------|
| | l_i Length of Insulation [m] | 0.015 |
| | Cp_i Specific heat [J/kg K] | 6.24 |
| | | 15 |

Thermal balance equation for the solar panel

$$m_{pv} Cp_{pv} \frac{T_{pv}^t - T_{pv}^{t-\Delta t}}{\Delta t} = -h_{conv(pv \rightarrow a)} S_{pv} (T_{pv} - T_a) - h_{rad(pv \rightarrow sk)} S_{pv} (T_{pv} - T_{sk}) - h_{cond(pv \rightarrow abst)} S_{pv} (T_{pv} - T_{abst}) + GS_{pv} \alpha_{pv} \quad (7)$$

Where m_{pv} is given by:

$$m_{pv} = \rho_{pv} l_{pv} S_{pv} \quad (8)$$

The heat transfer coefficient by convection between the solar panel and air is given by: [46]

$$h_{conv(pv \rightarrow a)} = \frac{N_u \lambda_{air}}{l_{pv}} \quad (9)$$

For laminar airflow $Re < 5 \cdot 10^5$, $10 \gg Pr \gg 0.5$, the N_u relation is given by:

$$N_u = 0.664 Re_l^{0.5} Pr^{1/3} \quad (10)$$

$$Re = \frac{\nu \rho_{air} l_{pv}}{\mu_{air}} \quad (11)$$

And the heat transfer coefficient by radiation between the solar panel and the sky is:

$$h_{rad(pv \rightarrow sk)} = \varepsilon \sigma (T_{pv}^2 + T_{sk}^2) (T_{pv} + T_{sk}) \quad (12)$$

Sky temperature T_{sk} is given by [47]:

$$T_{sk} = 0.0552 (T_a)^{1.5} \quad (13)$$

Where:

T_a is the ambient air temperature.

The heat transfer coefficient by conduction between the solar panel and the absorbing tube is:

$$h_{cond(pv \rightarrow abst)} = \frac{\lambda_{pv}}{e_{pv}} \quad (14)$$

The Thermal Balance Equation for the Absorbing Tube

$$m_{abst} Cp_{abst} \frac{T_{abst}^t - T_{abst}^{t-\Delta t}}{\Delta t} = -h_{cond(abst \rightarrow pv)} S_{abst} (T_{abst} - T_{pv}) - h_{conv(abst \rightarrow f)} S_{abst} (T_{abst} - T_f) - h_{cond(abst \rightarrow i)} S_{abst} (T_{abst} - T_i) \quad (15)$$

The mass of the absorber tube m_{abst} , is given by:

$$m_{abst} = \rho_{abst} L S_{abst} \quad (16)$$

The heat transfer coefficient by conduction between the absorber tube and the solar panel:

$$h_{cond(abst \rightarrow pv)} = \frac{\lambda_{abst}}{e_{pv}} \quad (17)$$

The heat transfer coefficient by convection between the absorber tube and the fluid:

$$h_{conv(abst \rightarrow f)} = \frac{N_u \lambda_f}{D} \quad (18)$$

For laminar flow of water $Re \leq 2300$, the following Nusselt number N_u expression is given: [47]

$$N_u = 4.36 \quad (19)$$

$$h_{cond(abst \rightarrow i)} = \frac{\lambda_i}{e_i} \quad (20)$$

The Thermal Balance Equation for the Fluid:

$$\dot{m}_f C p_f (T_f^t - T_f^{t-\Delta t}) = -h_{conv(f \rightarrow abst)} S_{abst} (T_f - T_{abst}) \quad (21)$$

Where S_{abst} is the lateral surface area of the absorber tube:

$$S_{abst} = \pi D L \quad (22)$$

Heat Transfer Coefficient by Convection:

$$h_{conv(f \rightarrow abst)} = \frac{N_u \lambda_f}{D} \quad (23)$$

The Thermal Balance Equation for the Insulation:

$$m_i C p_i \frac{T_i^t - T_i^{t-\Delta t}}{\Delta t} = -h_{cond(i \rightarrow abst)} S_i (T_i - T_r) - h_{conv(i \rightarrow a)} S_i (T_i - T_a) \quad (24)$$

The mass of the Insulation m_i , is given by:

$$m_i = \rho_i l_i S_i \quad (25)$$

The heat transfer coefficient by conduction between Insulation and the absorber tube:

$$h_{cond(i \rightarrow abst)} = \frac{\lambda_i}{e_i} \quad (26)$$

The heat transfer coefficient by convection between the Insulation and the ambient:

$$h_{conv(i \rightarrow a)} = \frac{N_u \lambda_{air}}{l_i} \quad (27)$$

For laminar airflow, the Nusselt number is given by:

$$N_u = 0.664 Re_i^{0.5} Pr^{1/3} \quad (28)$$

Thermal Efficiency Equation:

to calculate the thermal efficiency we use the results of test data for different parameters according to Equation: [48]

$$\eta_{th} = \frac{\dot{m}_f C p_f (T_{f out} - T_{f in})}{G S_{pv}} \quad (29)$$

$T_{f in}$ and $T_{f out}$ present the temperatures at the inlet and outlet of the Water channel respectively, \dot{m}_f and $C p_f$ the mass flow rate and specific heat capacity of Water . G is the solar radiation .

Simulation:

Numerical simulation was conducted using MATLAB. For the electrical part, Simulink was used, while for the thermal part, the thermal balance equations were solved in MATLAB using the Gauss-Seidel method. The solar radiation was calculated every 15 minutes from 7 AM to 7 PM.

Discussion of Results:

The Effect of Radiation Intensity and Temperature:

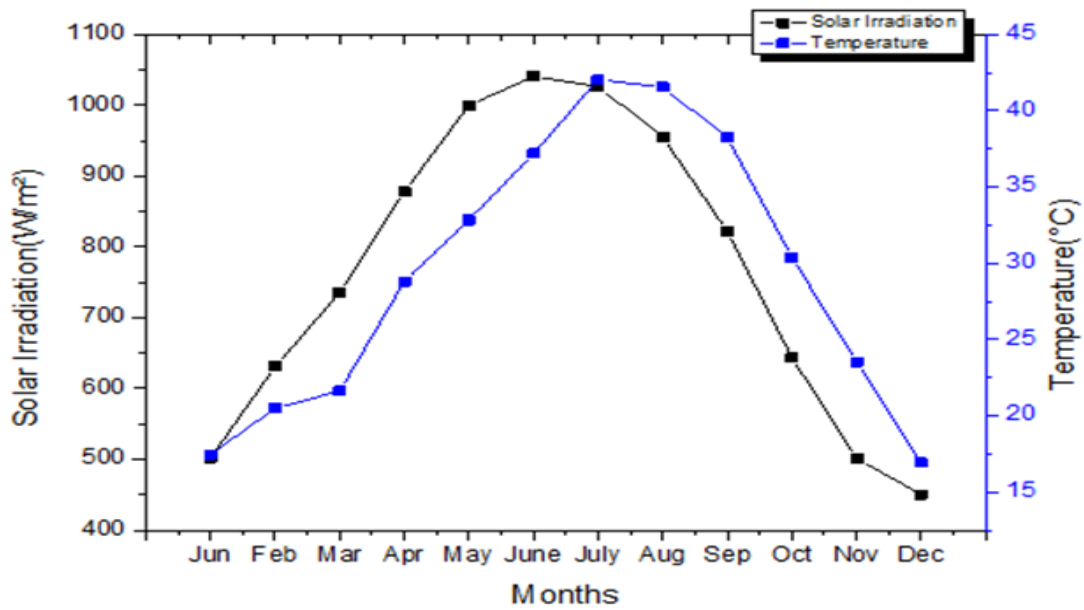


Figure 4: The changes in solar radiation and the temperature of the solar panel during the year.

Curve (4) represents the changes in solar radiation and solar panel temperature by months for the Ouargla region, where we observe the highest values of solar

radiation and temperature during the summer months, significantly reducing the efficiency of the cell, hence the need for hybridization.

Power and Current Throughout Each Month:

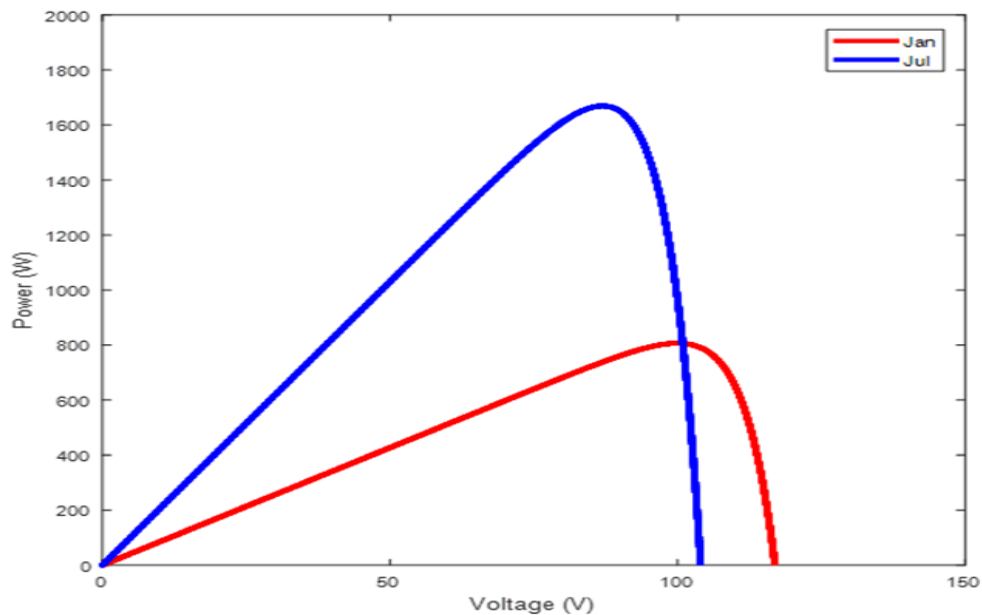


Figure 5: The changes in power with respect to voltage for a summer day and a winter day.

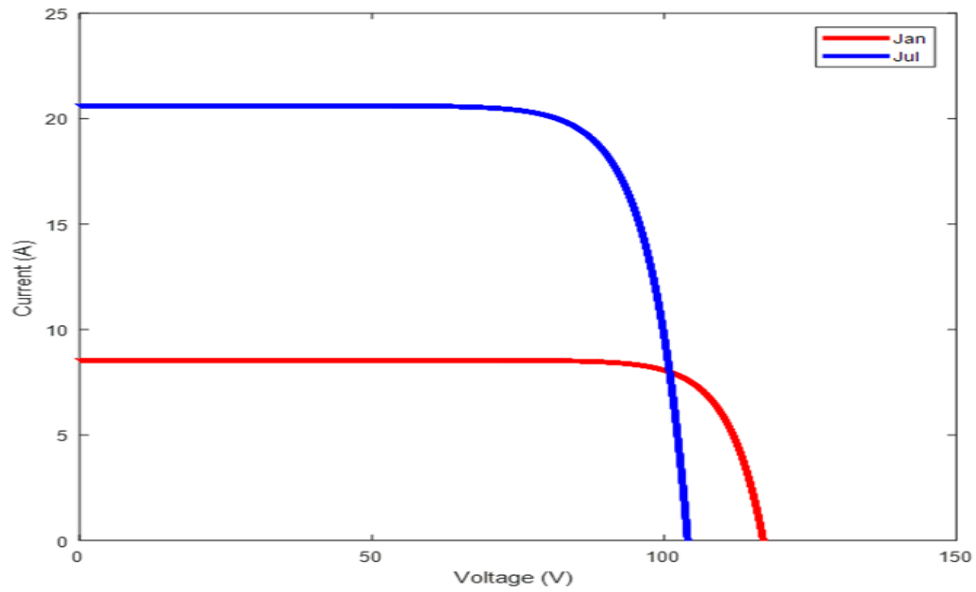


Figure 6: The changes in current with respect to voltage for a summer day and a winter day.

Curves (5 and 6) represent the changes in power and current with respect to voltage on July 15th and January 15th, where we notice that the power reached 1700 watts

on a summer day, while it was 800 watts on a winter day, indicating that power increases with increased solar radiation.

Temperature of the Solar Panel:

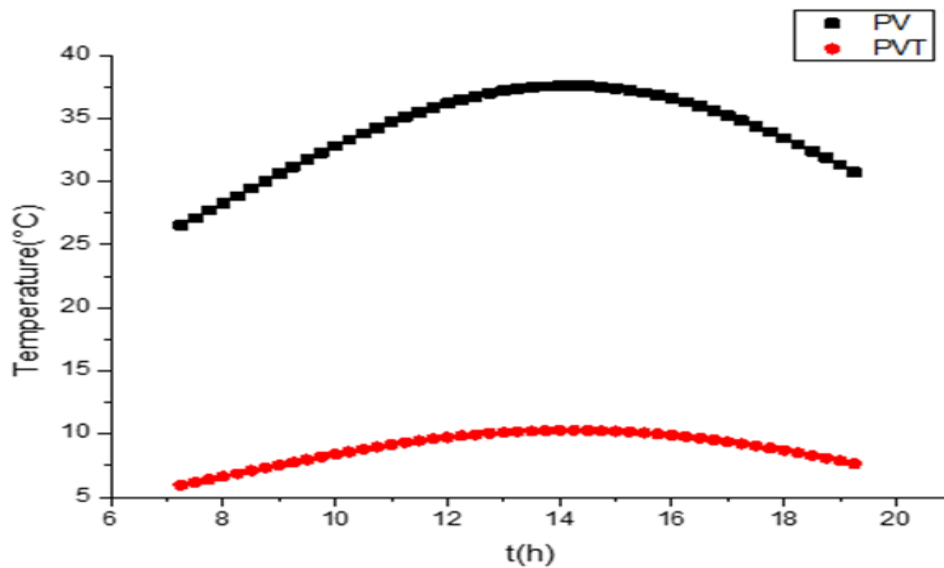


Figure 7: The changes in the temperature of the solar panel before and after hybridization on a winter day (January 15th).

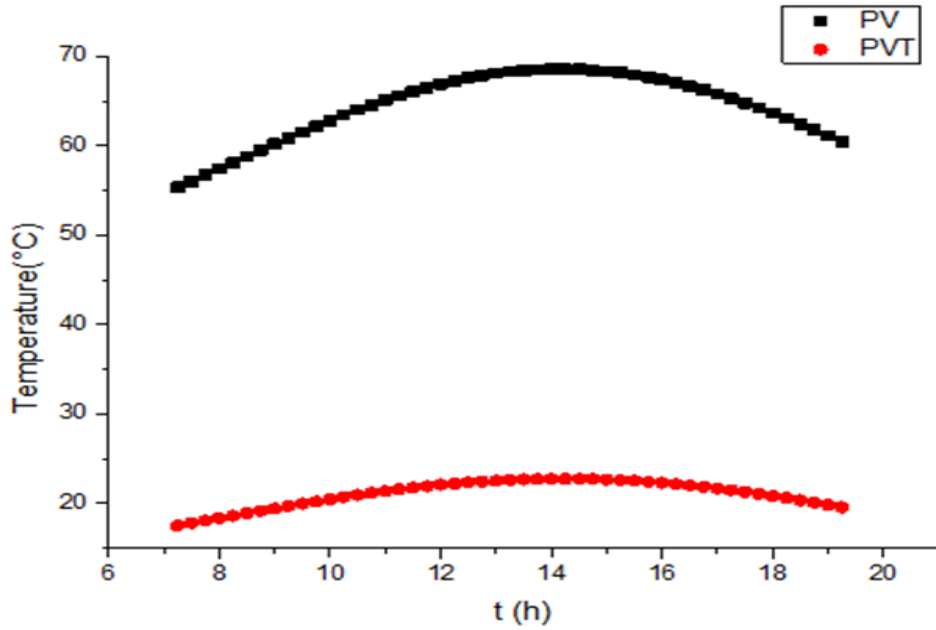


Figure 8: The changes in the temperature of the solar panel before and after hybridization on a summer day (July 15th).

Curves (7 and 8) represent the changes in the solar panel's temperature before and after hybridization over time during a winter day (January 15th) and a summer

day (July 15th), where we observe a decrease in temperature by 20°C on a winter day and 30°C on a summer day after hybridization.

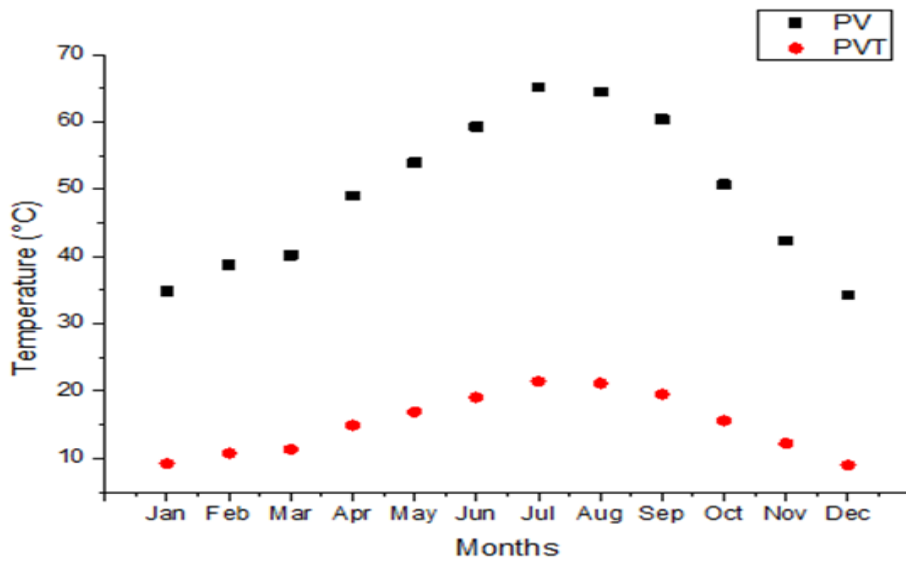


Figure 9: The changes in the solar panel's temperature before and after hybridization throughout the year.

Curve (9) represents the changes in the solar panel's temperature before and after hybridization over time during the year, where we observe a significant decrease

in temperature, especially during the summer months, leading to an increase in cell efficiency.

Electrical Efficiency:

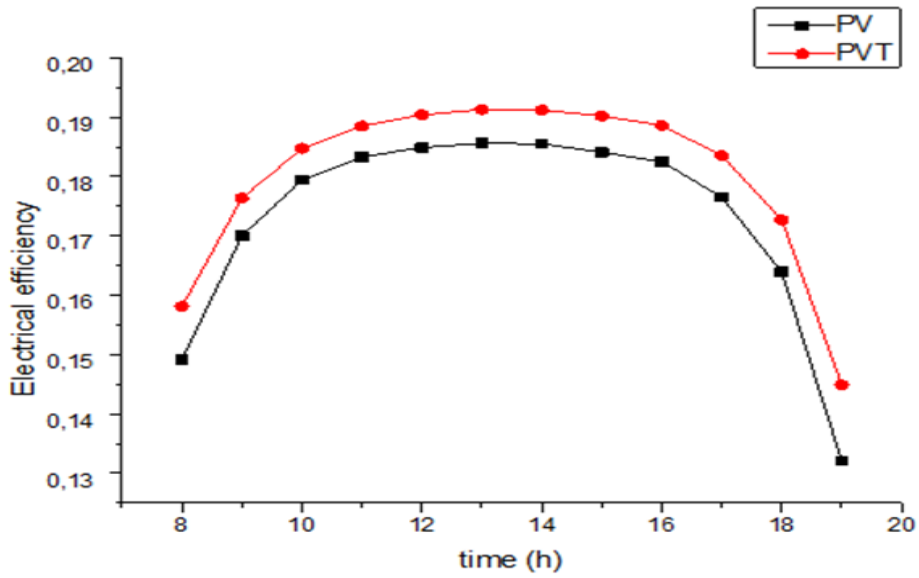


Figure 10: The changes in the electrical efficiency of the solar panel before and after hybridization during January.

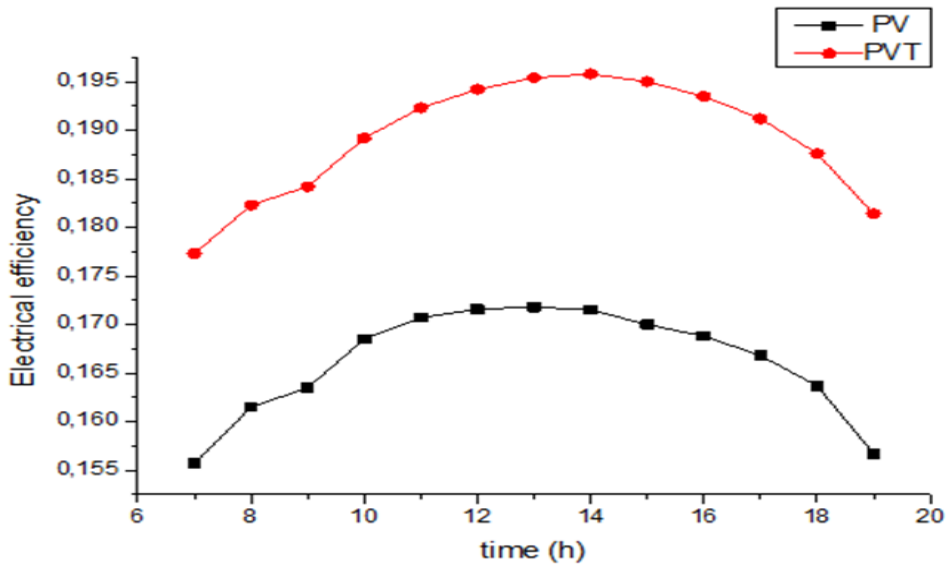


Figure 11 : The changes in the electrical efficiency of the solar panel before and after hybridization during July.

Curves (10 and 11) represent the changes in electrical efficiency over time before and after hybridization on a summer day (July 15th) and a winter day (January 15th),

where we notice an increase in efficiency by 1% on a winter day and 2.5% on a summer day.

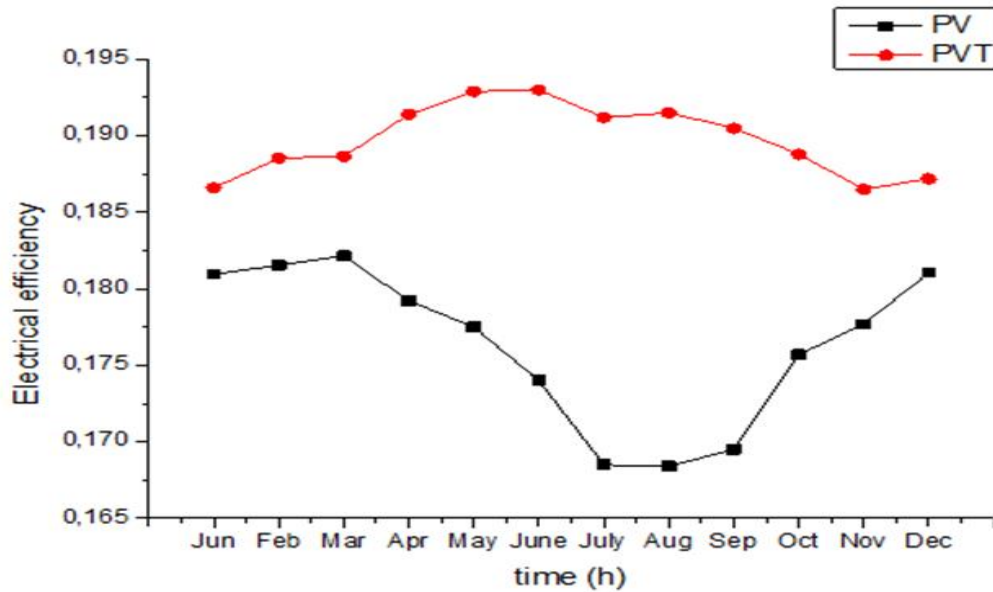


Figure 12 : The changes in the electrical efficiency of the solar panel before and after hybridization throughout the year.

Curve (12) represents the changes in efficiency over time before and after hybridization during the year,

where we notice a significant and evident increase in efficiency, especially during the summer months.

Temperature of the Exiting Water:

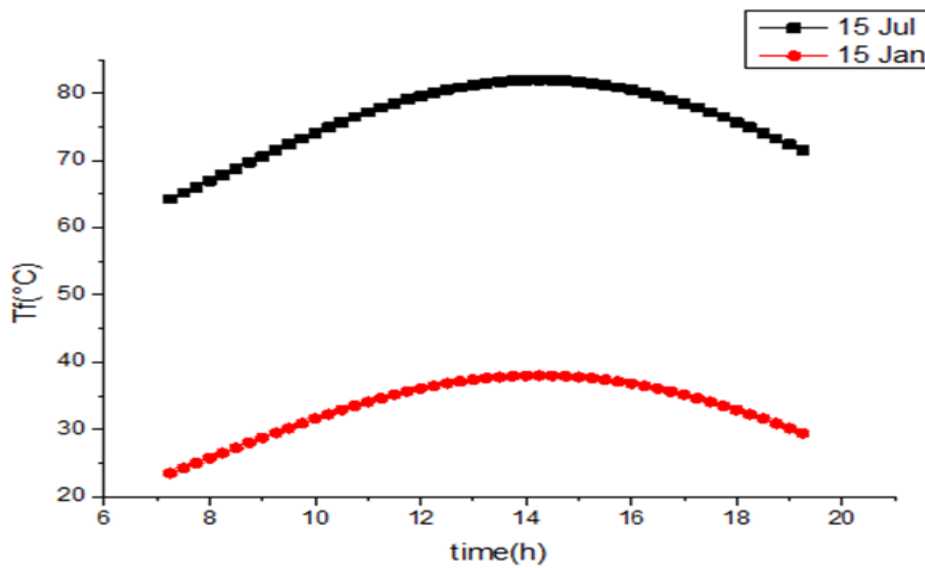


Figure 13 : the changes in the temperature of the exiting water on a summer day and a winter day.

Curve (13) represents the changes in the temperature of the exiting water, where we notice that the water

temperature reached 85°C on a summer day while it was 40°C on a winter day.

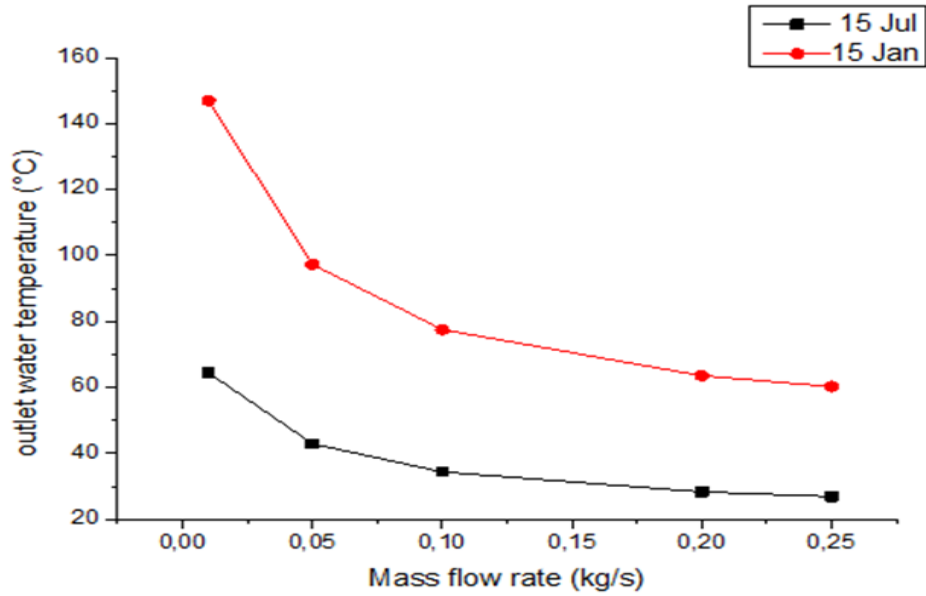


Figure 14 : the changes in the temperature of the exiting water as a function of the flow rate on a summer day and a winter day.

Curve (14) represents the changes in the temperature of the exiting water with respect to the flow rate on a summer day and a winter day, where we notice that as

the water flow increases, the temperature of the exiting water decreases.

Thermal Efficiency:

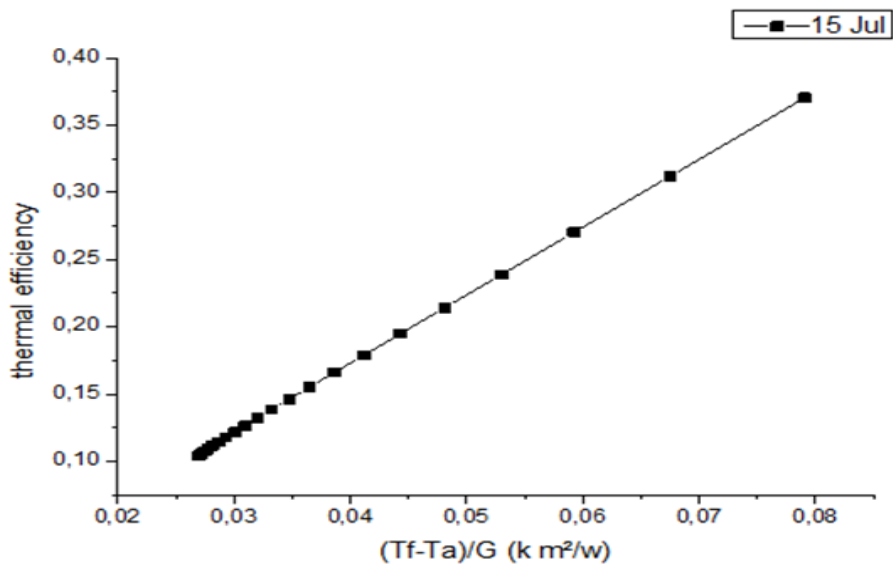


Figure 15 : The changes in thermal efficiency with respect to the temperature difference on a summer day.

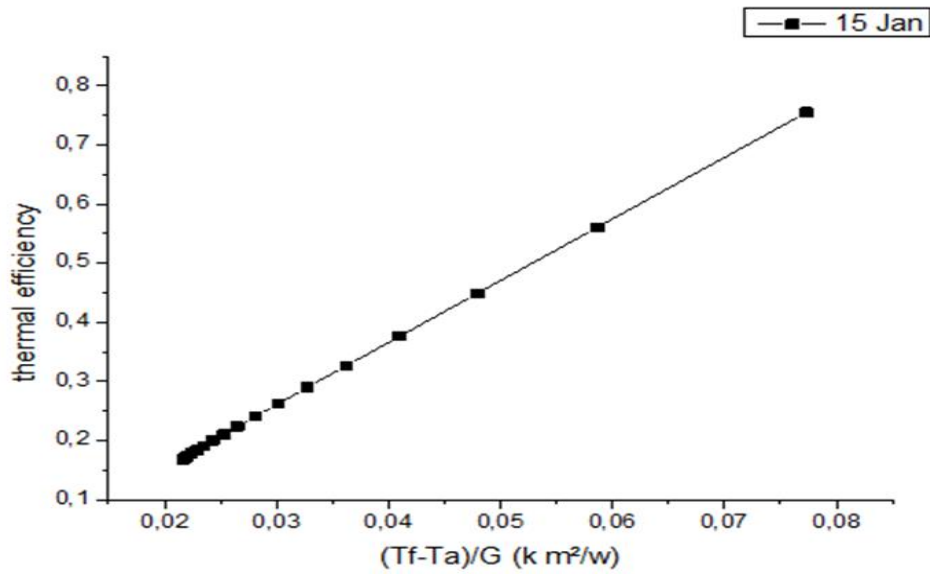


Figure 16 : The changes in thermal efficiency with respect to the temperature difference on a winter day.

Curves (15, 16) represent the changes in thermal efficiency with respect to the temperature difference for

both a summer day and a winter day, indicating that as the difference increases, so does the thermal efficiency.

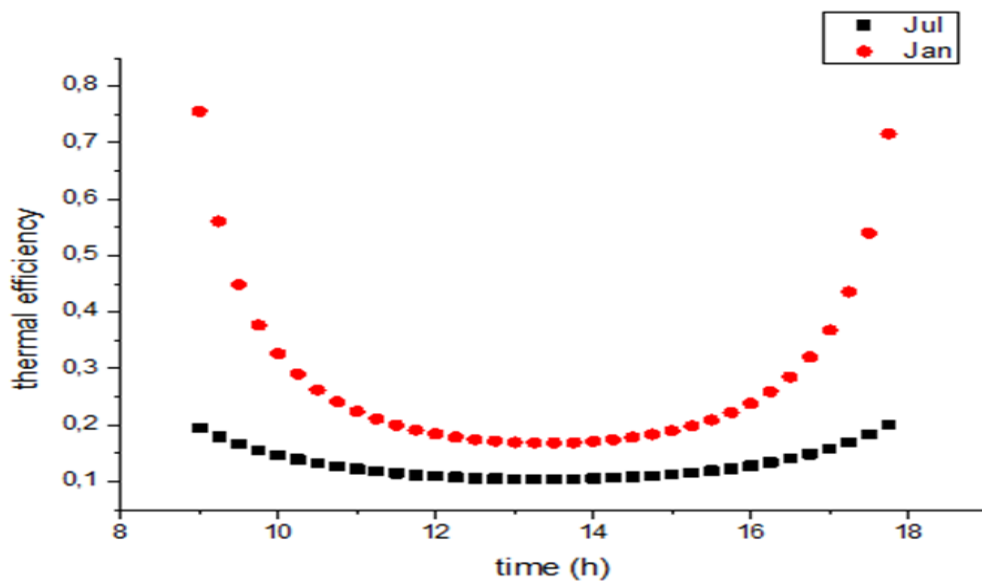


Figure 17: The changes in thermal efficiency over time on both a summer and a winter day

Curve (17) represents the changes in thermal efficiency over time on both a summer and a winter day, noting that the maximum value of thermal efficiency reached 75% on a summer day while it was 22% on a winter day, and the thermal efficiency reaches its minimum value around noon.

Validation :

we compared The numerical simulation results obtained by the present PV/T model with other numerical simulation and experimental results. of the Electrical and thermal efficiency, the temperature of the solar panel before and after hybridization and the Outlet water temperature. Table 4 shows comparison , they are in good concordance with the data given by Billel Boumaaraf et al. [49]

Table 4 comparison of our results with previous results

| parameter | Billel Boumaaraf et al | Present work |
|---|------------------------|--------------|
| Electrical efficiency | 7% | 17% |
| temperature of the solar panel before hybridization | 65°C | 65°C |
| temperature of the solar panel after hybridization | 30°C | 25 |
| thermal efficiency | 70% | 75% |
| Outlet water temperature | 70°C | 80°C |

Conclusion:

This study conducted a theoretical analysis using MATLAB/Simulink on hybrid photovoltaic-thermal systems, describing an accurate model of the equivalent circuit for a single diode of the photovoltaic module and applying the thermal balance equations for generating both electrical and thermal energy.

- For the PV system, the power produced by the solar panel was 700W with an efficiency of 18% on a winter day, while on a summer day, the power reached 1700W with an efficiency of 17%.
- For the PVT system, the efficiency was 19% on a winter day, while on a summer day, it reached 19.5%.
- After applying the hybrid system, we found that the temperature variation of the PV panel before and after hybridization can reach up to 30°C on a summer day.
- On a winter day, the electrical efficiency was improved by 1% through the PVT system.
- On a summer day, the electrical efficiency was improved by 2.5% through the PVT system.
- The need for the PVT system becomes critical during the summer due to the region's hot climate.
- The thermal efficiency of the PVT system reached 75% on a winter day and 22% on a summer day.
- The fluid temperature in the heat exchanger reaches 85°C in summer and 40°C in winter, suitable for thermal applications.
- Increasing the fluid flow in the heat exchanger leads to a decrease in fluid temperature.
- Higher fluid temperatures can be achieved, making it suitable for industrial uses in larger PVT systems.
- The greater the temperature difference between the water temperature and the air temperature divided by the radiation, the higher the electrical efficiency.

- PV/T systems can fully meet the demand for electricity and heat for buildings, significantly reducing carbon dioxide emissions.
- PV/T systems are reliable and operate in a noise-free environment. The lifespan of these systems is about 20-30 years with negligible maintenance costs.

References:

[1] "Roadmap, PVT," *a European guide for the development and market introduction of PV-thermal technology*, 2006. <http://www.pvtforum.org/index.html>

[2] M. S. Browne MC, Norton B, "tion of a photovoltaic/thermal collec_tor with PCM," *Sol Energy*, vol. 133, pp. 533–48, 2016, doi: <https://doi.org/10.1016/j.solener>.

[3] N. ton B. Hasan A, McCormack SJ, Huang MJ, Sarwar J, "Increased photovoltaic performance through temperature regulation by phase change materials: materials comparison in different climates," *Sol Energy*, vol. 115, pp. 264–76., 2015, doi: <https://doi.org/10.1016/j>.

[4] B. Odeh S, "Improving photovoltaic module using water cooling," *Taylor Fr*, 7632, 2017, doi: <https://doi.org/10.1080/01457630802529214>.

[5] U. Naseem Abbas, Muhammad Bilal Awan, Moham med Amer, Syed Muhammad Amard and A. T. Hafiz Muhammad Ali h, Nida Zahra, MuzamilHus sain, Mohsin Ali Badshah, "Ap_plications of nanofluids in photovoltaic thermal sys_tems: A review of recent advances," *Physica A*, vol. 536, pp. 122–513, 2019.

[6] R. S. Ahmed S. Abdelrazik, FA Al-Sulaimana and R. Ben Mansoura, "A review on recent devel_opment for the design and packaging of

- hybrid photovoltaic/thermal (PV/T) solar system,” *Renew. Sustain. Energy Rev.*, vol. 95, pp. 110–129., 2018.
- [7] “Solar heat worldwide,” *Int. Energy Agency Sol. Heat. Cooling Program.*, 2016, doi: www.iea-shc.org/data/sites/1/publications/Solar-Heat-Worldwide.
- [8] A. B. K. Y. Khanjari, F. Pourfayaz, “Numerical investigation on using of nanofluid in a water-cooled photovoltaic thermal system,” *Energy Convers. Manag.*, vol. 122, pp. 263–278, 2016.
- [9] T. G. Boer KW, “Solar conversion under consideration of energy and entropy,” *Sol Energy*, vol. 74, no. 525–8, 2003.
- [10] A. R. Garg HP, “Some aspects of a PVT collector/forced circulation flat plate solar water heater with solar cells,” *Energy Convers Manag.*, vol. 36, no. 87–99, 1995.
- [11] D. V. DW., “Design of a photovoltaic thermal combi-panel,” 1998.
- [12] V. S. hoven Zondag HA, De Vries DW, Van Helden WGJ, Van Zolingen RJC and AA, “The thermal and electrical yield of a PV–thermal collector ;72:113–28,” *Sol Energy*, vol. 72, no. 113–28, 2002.
- [13] K. SA, “Use of TRNYSYS for modeling and simulation of a hybrid PV– thermal solar system for Cyprus,” *Renew. Energy*, vol. 23, no. 247–60, 2001.
- [14] S. M. Tiwari A, “Performance evaluation of solar PVT system: an experimental validation,” *Sol Energy*, vol. 80, no. 751–9, 2006.
- [15] T. Y, “Aspects and improvements of hybrid photovoltaic thermal solar energy systems,” *Sol Energy*, vol. 81, no. 1117–31, 2007.
- [16] A. M. Shahsavari A, “Experimental investigation and modeling of a direct coupled PVT air collector,” *Sol Energy*, vol. 84, no. 1938–58, 2010.
- [17] J. H. Bakar NAM, Othman M, Mahadzir HD, Manaf NA, “Design concept and mathematical model of a bi-fluid photovoltaic thermal (PVT) solar collector,” *Renew. Energy*, vol. 67, no. 153–64, 2014.
- [18] T. G. Vats K, Tomar V, “Effect of packing factor on the performance of a building integrated semitransparent photovoltaic thermal (BISPVT) system with air duct,” *Energy Build*, vol. 53, no. 159–65., 2012.
- [19] T. S. Tyagi VV, Pandey AK, Kaushik SC, “Thermal performance evaluation of a solar air heater with and without thermal energy storage,” *J Therm Anal Calorim*, vol. 107, no. 1345–52, 2012.
- [20] M. A. Touafek K, Mourad H, “Design and modeling of a photovoltaic thermal collector for domestic air heating and electricity production,” *Energy Build*, vol. 59, no. 21–8, 2013.
- [21] A.-A. M. Amori KE, “Field study of various air based photovoltaic/ thermal hybrid solar collectors,” *Renew. Energy*, vol. 63, no. 402–14, 2014.
- [22] K. I. Al-Alili A, Hwang Y, Radermacher R, “A high efficiency solar air conditioner using concentrating photovoltaic/thermal collectors,” *Appl Energy*, vol. 93, no. 138–47, 2012.
- [23] S. Y. Li G, Pei G, Yang M, Ji J, “Optical evaluation of a novel static incorporated compound parabolic concentrator with photovoltaic/thermal system and preliminary experiment,” *Energy Convers Manag.*, vol. 85, no. 204–11, 2014.
- [24] J. J. Gang P, Huide F, Huijuan Z, “Performance study and parametric analysis of a novel heat pipe PV/T system,” *Energy*, vol. 37, no. 384–95, 2012.
- [25] X. J. Zhang X, Zhao X, Shen J, Hu X, Liu X, “Design, fabrication and experimental study of a solar photovoltaic/loop-heat-pipe based heat pump system,” *Sol Energy*, vol. 97, no. 551–68, 2013.
- [26] A. I. Moradgholi M, Nowee SM, “Application of heat pipe in an experimental investigation on a novel photovoltaic/thermal (PV/T) system,” *Sol Energy*, vol. 107, no. 82–8, 2014.
- [27] et al Ji J, “Distributed dynamic modelling and experimental study of PV evaporator in a PVT solar-assisted heat pump,” *Int J Heat Mass Transf.*, vol. 52, no. 1365–11373.
- [28] M. Alktrane and P. Bencs, “Applications of nanotechnology with hybrid

- photovoltaic/thermal systems: A review,” *J. Appl. Eng. Sci.*, vol. 19, no. 2, pp. 292–306, 2021, doi: 10.5937/jaes0-28760.
- [29] V. M. K. R. B. Ganvir, P. V. Walke, “Heat transfer characteristics in nanofluid - A review,” *Renewable Sustain. energy Rev.*, vol. 75, no. 451–460, 2017.
- [30] U. Naseem Abbas, Muhammad Bilal Awan, Moham med Amer, Syed Muhammad Ammar and A. T. Hafiz Muhammad Ali h, Nida Zahra, MuzamilHus sain, Mohsin Ali Badshah, “Ap_plications of nanofluids in photovoltaic thermal sys_tems: A review of recent advances,” *Physica A*, vol. 536, no. 122–513, 2019.
- [31] A. B. K. Y. Khanjari, F. Pourfayaz, “Numerical investigation on using of nanofluid in a water-cooled photovoltaic thermal system,” *Energy Convers. Manag.*, vol. 122, no. 263–278, 2016.
- [32] D. H. Bajestan EE, Moghadam MC and W. S, “Experimental and numerical investigation of nanofluids heat transfer character_istics for application in solar heat exchang,” *Int J Heat Mass Transf*, vol. 92, no. 1041–52, 2016.
- [33] A. . Hussein, “Applications of nanotechnology in renewable energies-A comprehensive overview and understanding. *Renew. Sustain., Energy Rev*, vol. 42, no. 460–476, 2015.
- [34] T. G. Dubey S, “Thermal modeling of a combined system of photovoltaic thermal (PV/T) solar water heater,” *Sol Energy*, vol. 82, no. 602–12, 2008.
- [35] T. G. Mishra RK, “Energy and exergy analysis of hybrid photovoltaic thermal water collector for constant collection temperature mode,” *Sol Energy*, vol. 90, no. 58–67, 2013.
- [36] T. Va and R. Sekhar, “Hybrid Photovoltaic / Thermal (PVT) Collector Systems With Different Absorber Con_fi_gurations For Thermal Management – A Review,” no. March 2022, 2021, doi: 10.1177/0958305X211065575.
- [37] S. D. Prasetyo, A. R. Prabowo, and Z. Arifin, “Heliyon The use of a hybrid photovoltaic / thermal (PV / T) collector system as a sustainable energy-harvest instrument in urban technology,” *Heliyon*, vol. 9, no. 2, p. e13390, 2023, doi: 10.1016/j.heliyon.2023.e13390.
- [38] Z. Zhang, H., Ma, X., You, S., Wang, Y., Zheng, X., Ye, T. and S. W., Wei, “Mathematical modeling and performance analysis of a solar air collector with slit-perforated corrugated plate. J,” *Sol Energy*, vol. 167, no. 147–157, 2018.
- [39] Vinod, R. Kumar, and S. K. Singh, “Solar photovoltaic modeling and simulation: As a renewable energy solution,” *Energy Reports*, vol. 4, pp. 701–712, 2018, doi: 10.1016/j.egy.2018.09.008.
- [40] G. Data and S. Tables, “PS1800 Centrifugal Pumping Systems,” no. Aisi 316.
- [41] H. Bellia, “A detailed modeling of photovoltaic module using MATLAB,” *NRIAG J. Astron. Geophys.*, 2014, doi: 10.1016/j.nrjag.2014.04.001.
- [42] B. Alsaid, “Modeling and Simulation of Photovoltaic Cell / Module / Array with Two-Diode Model,” vol. 1, no. 3, pp. 6–11, 2012.
- [43] E. Villalva, M.G., Gazoli, J.R., Ruppert Filho, “Comprehensive approach to modeling and simulation of photovoltaic arrays. *IEEE Trans., Power Electron*, vol. 24 (5), no. 1198–1208, 2009, doi: <http://dx.doi.org/10.1109/TPEL.2009.2013862>.
- [44] P. . Lyden, S., Haque, M.E., Gargoom, A., Negnevitsky, M., Muoka, “Modeling and parameter estimation of photovoltaic cell,” in *Power Engineering Confer_ence, AUPEC. IEEE*, 2012, pp. 1–6.
- [45] N. Khenfer, B. Dokkar, and M. Taher, “Overall efficiency improvement of photovoltaic - thermal air collector : numerical and experimental investigation in the desert climate of Ouargla region,” *Int. J. Energy Environ. Eng.*, 2020, doi: 10.1007/s40095-020-00353-1.
- [46] O. KS, “Thermal performance of solar air heaters: mathematical model and solu_tion procedure,” *Sol Energy*, vol. 55, no. 2, pp. 93–109, 1995, doi: [https://doi.org/10.1016/0038-092X\(95\)00021-I](https://doi.org/10.1016/0038-092X(95)00021-I).
- [47] Z. S. Chang W, Wang Y, Li M, Luo X, Ruan Y, Hong Y, “The theoretical and experimental research on thermal performance of solar air collector with finned absorber,” *Energy Procedia*, vol. 70, no. 13–22, 2015, doi: <https://doi.org/10.1016/j.egypro.2015.02.092>.
- [48] C. T. and H. W. Ji J., “Dynamic Performance of

Hybrid Photovoltaic/Thermal Collector Wall in Hong Kong,” *Build. Environ.*, vol. 38, no. 11, pp. 1327 – 1334, 2003.

- [49] B. Boumaaraf, H. Boumaaraf, M. E. A. Slimani, S. Tchoketch_Kebir, M. S. Ait-cheikh, and K. Touafek, “Performance evaluation of a locally

modified PV module to a PV/T solar collector under climatic conditions of semi-arid region,” *Math. Comput. Simul.*, vol. 167, no. September, pp. 135–154, 2020, doi: 10.1016/j.matcom.2019.09.013.

Annexes

| Nomenclature | |
|-----------------|---|
| PV/T | Photovoltaic/thermal |
| PV | Photovoltaic |
| IPVTS | integrated photovoltaic and thermal solar energy system |
| BIPV/T | Building-integrated photovoltaic/thermal |
| PCM | phase change material |
| CPC-PV/T | concentrator Photovoltaic/thermal system |
| PVT-SAHP | Photovoltaic/thermal solar assisted heat pump |
| STC | Standard Test Conditions |

| Symblos | | | |
|----------|--|----------|--|
| p_m | Maximum power [W] | I_{ph} | Photocurrent of a solar PV cell generated due to solar irradiation [A] |
| v_m | Maximum power voltage [V] | P_r | Prandtl number |
| I_m | Maximum power current [A] | T | Temperature [°C] |
| v_{oc} | Open circuit voltage [V] | m | mass [kg] |
| I_{sc} | Short-circuit current at STC [A] | I | Output current from the PV panel [A] |
| N_p | Number of cells connected in parallel | p_m | Maximum power [W] |
| A | Ideality factor of the diode | R_e | Reynolds number |
| I_s | Saturation current [A] | N_u | Nusselt number |
| N_s | Number of cells connected in series | C_p | Specific heat [J/kg K] |
| I_{rs} | G Solar irradiance [W/m ²] Reverse saturation current [A] | h | Heat transfer coefficient [W/m ² K] |

| | | | |
|-----------|---|------------------------|--|
| E_g | Forbidden Energy band gap, for silicon = 1.1 eV | V | Output voltage from the PV panel [V] |
| G_{ref} | Solar Irradiance at STC [W/m ²] | t | Time [s] |
| K_i | Temperature coefficient of Isc cell short circuit current [0.005254 A/°C] | N I_0 S_{pv} | Total Number of Cells Current of a Single Cell Total Area of the Solar Panel |
| T_{ref} | Reference temperature [°C] | \dot{m} | Mass flow rate [kg/s] |
| T_r | Reference temperature [K] | P_0 | Power of a Single Solar Cell [W] |
| T_o | Real-time temperature [K] | V_0 | Voltage of a Single Cell [V] |
| K | Boltzmann's constant = 1.380×10^{-23} J/K | S | Area of a Single Cell [m ²] |
| R_s | Series resistance of the PV module [Ω] | v_m | Maximum power voltage [V] |
| q | Charge of an electron = 1.602×10^{-19} C | [V] | V_M operating voltage of the pump |
| I_d | Diode current [A] | | |

| Greek symbols | |
|---------------|---|
| α | Absorption coefficient |
| ε | Emissivity |
| η | Efficiency |
| λ | Thermal conductivity [w m ⁻¹ k ⁻¹] |
| σ | Stefan-Boltzmann constant= 5.67010^{-8} [W/m ² K ⁴] |
| ρ | Density [kg/m ³] |
| μ | Dynamic viscosity [kg m ⁻¹ s ⁻¹] |

| Subscripts | |
|-------------|----------------|
| <i>el</i> | Electrical |
| <i>pv</i> | PV glass-cover |
| <i>abst</i> | Absorber Tube |
| <i>f</i> | Fluid water)(|
| <i>i</i> | Insulation |

| | |
|-------------|------------|
| | |
| <i>a</i> | Ambient |
| <i>cond</i> | Conduction |
| <i>conv</i> | Convection |
| <i>rad</i> | Radiation |
| <i>th</i> | Thermal |
| <i>out</i> | Outlet |
| <i>in</i> | Inlet |